ESRF	**Experiment title: Thin Film Structure of Semiconductor Donor-Acceptor Block Copolymers for Organic Solar Cells**	**Experiment number**: **SC-3794**
Beamline: ID10B	**Date of experiment**: from: 07.09.2013 to: 10.09.2013	**Date of report**: 12.03.2014
Shifts: 9	**Local contact(s)**: Oleg Konovalov	*Received at ESRF:*

Names and affiliations of applicants (* indicates experimentalists):

Applicants: Thomas Thurn-Albrecht[1], Gaurav Gupta[1]*, Matthias Fischer[1]*, Mukundan Thelakkat[2]

Additional experimentalists: Jens Balko[1]*, David Heinrich[2]*, Martin Hufnagel[2]*

[1] Martin Luther University Halle, Institute of Physics, 06120 Halle, Germany

[2] University of Bayreuth, Applied Functional Materials, Macromolecular Chemistry I, 95447 Bayreuth, Germany

Report:

Overview and Scientific Questions Addressed

Within the beamtime we investigated self-assembling donor-acceptor materials which are used to optimize bulk heterojunction solar cells based on ordered, oriented block copolymers. In order to achieve percolating pathways for charge transport, it is critical to control the orientation of the resulting donor-acceptor nanostructures by either external fields or other means such as solvent vapor annealing.
Here we studied the resulting nanostructures as well as the crystalline structures by thin film X-ray scattering in grazing incidence geometry (GISAXS, GID) as well as in specular condition. We aim for a perpendicular orientation of the donor-acceptor nanostructures with respect to the substrate. The experimental results, indeed, indicate an orientation effect achieved by means of an electric field as well as solvent vapor annealing. However, the desired vertical orientation of the nanostructures could not yet be verified. In addition we performed measurements which allow the determination of the orientation distribution function of the crystalline domains within the nanostructures (GID, specular condition).
Complementary, we did experiments on a novel block copolymer, synthesized recently within the project, and investigated P3HT homopolymers with the aim to observe the SAXS signal due to the semicrystalline morphology.

Experimental

All measurements were done at a photon energy of 8 keV. The beam was collimated with two slits to a lateral size of 0.3 mm. An additional guard slit directly in front of the sample reduced the parasitic scattering from the first slits. The vertical slit collimated the beam to a height of 0.015 mm. Thin film samples prepared on SiO_2/Si substrates (15 x 15 mm²) were placed on an horizontal sample stage (Huber 5202) and were measured in air. The scattered intensity was recorded using an PILATUS 300k area detector (Dectris) placed on a trail with an active area of 34 x 27 cm² (619 x 487 pixels) and a pixel size of 172 µm.
Grazing incidence small angle X-ray scattering (GISAXS) measurements were done with a sample to detector distance of 81.9 cm. The incident angle was at around 0.17° which is slightly above the critical angle of the organic films and below the critical angle of the substrate. Grazing incidence diffraction (GID) measurements were performed using the same incident angle and at a sample to detector distance of 29.3 cm. In order to get structural information not obtained with the GID pattern, we performed measurements using

the specular condition where the incident angle corresponds to half of the Bragg angle of a certain Bragg reflection. This measurement probes crystallographic planes which are exactly parallel to the substrate. The thin films were either crystallized by slowly cooling from the melt ('melt-crystallized') or treated by solvent-vapor annealing.

List of the Main Results

Here were only present a short summary of the results (table below). For a detailed description, we refer to the appendix A-E. Whereas treating the model sample with an E-field had an effect on the resulting orientation of the morphology the results for the solar cell material RL122 are not conclusive (App. A). Thin films treated by solvent-vapor annealing showed no clear GISAXS signal (App. B). However, we consider these results as preliminary due to the lack of understanding the structure formation during solvent-vapor annealing which at present is also under discussion in the literature. The additional experiments gave promising results (App. C-E)
Abbreviations are given in the following:

PS	…polystyrene
PPerAcr	…poly(perylene acrylate)
P3HT	…poly(3-hexyl thiophene)
PPCBM	…polystyrene copolymer grafted with phenyl-C61-butyric acid methyl ester
A-b-B	…block copolymer consisting of block A covalently bonded to block B

Sample (description)	App.	Results
MiS195 (PS-b-PPerAcr)	**A**	- melt-crystallized: phase separation confirmed, cylindrical domains parrallel to substrate - E-field: phase separation confirmed, orientation of cylindrical domains ambiguous
RL122 (P3HT-b-PPerAcr)	**A**	- melt-crystallized: phase separation confirmed, cylindrical domains parallel to substrate - E-field: no phase separation observed
RL95 (P3HT-b-PPerAcr) (the same material as RL122)	**B**	- solvent-vapor annealing: no phase separation with GISAXS observed maybe due to insufficient film thickness
RL95 (P3HT-b-PPerAcr)	**C**	- orientation distribution of crystallites can be studied by analysis of GID pattern
MH155 (P3HT-b-PPCBM)	**D**	- melt-crystallized: phase separation confirmed
RL22 (P3HT)	**E**	- clear GISAXS signal corresponding to the expected long period
SEP200 (P3HT)	**E**	- GISAXS signal is possibly to weak

Appendix A

For the electric field orientation experiments two materials were used, which are depicted in Figure 1. Both of them show a cylindrical phase separation of PS cylinders (MiS195) and P3HT cylinders (RL122) in a PPerAcr-matrix. The samples were prepared by spincoating on silicon substrates with a native SiO_2-Layer.

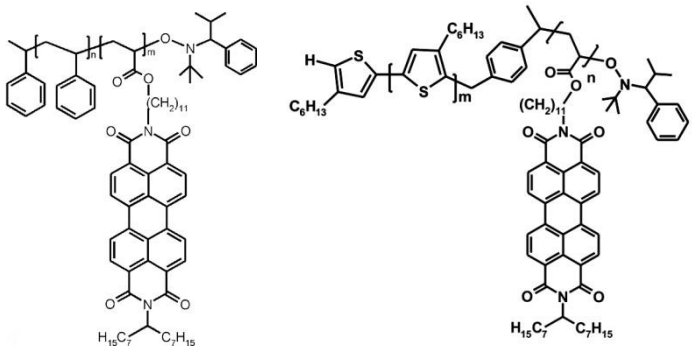

Figure 1: Chemical structures of the investigated materials for the electric field alignment. Polystyrene-*block*-poly(perylene acrylate) (PS-*b*-PPerAcr, MiS195) (left), poly(3-hexyl thiophene)-*block*-poly(perylene acrylate) (P3HT-*b*-PPerAcr, RL122)[1,2]

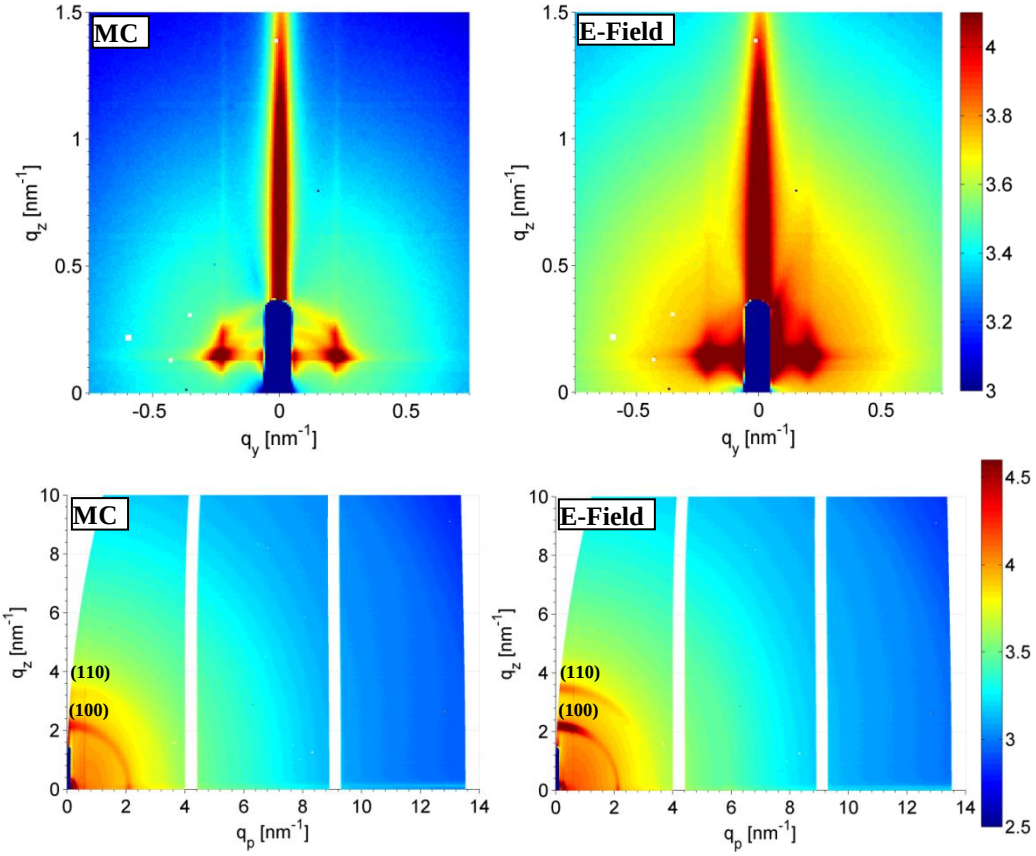

Figure 2: GISAXS (top) and GIWAXS (bottom) data (logarithmic scale) of MiS195 after melt crystallisation (left) and electric field treatment (right).

While for the application of the electric field the silicon substrate served as the bottom electrode, an aluminised Kapton film was used as top electrode with a 26 µm thick polydimethylsiloxane (PDMS) insulation layer in between. In order to orient the phases in the materials the samples were placed in nitrogen atmosphere and heated above their melting temperature while an AC-field was applied with a frequency of 50 Hz and a field strength of around 15 V/µm. In this state the samples stayed overnight before they were cooled down and the field was switched off. The electric field treated samples are compared to melt

[1] S. Hüttner, M. Sommer, M. Thelakkat: n-type organic field effect transistors from perylene bisimide block copolymers and homopolymers, Appl. Phys. Lett. 92, 093302, 2008
[2] S. Hüttner, J. M. Hodgkiss, M. Sommer, R. H. Friend, U. Steiner, M. Thelakkat, J. Phys. Chem. B 116, 10070, 2012

crystallised samples, where the samples were only heated above their melting temperature without applied electric field.
As can be seen in the upper GISAXS images shown in Figure 2 the MiS195 block copolymer shows a clear signal due to microphase separation in the melt crystallised state as well as after the electric field treatment, without a change in the position of the signal. Furthermore a ring can be observed in the melt crystallised sample, presumably indicating a fraction of not oriented material. After the application of the electric field the ring cannot be observed anymore, which could indicate that the morphology in the sample is the desired morphology of cylinders standing perpendicular to the substrate. However, due to the difficult interpretation of the data we conclude that studying a sample having a lamellar block copolymer morphology would be advantegous in order to distinguish between perpendicular and parallel structures. Also a change in the GIWAXS images can be observed. After the electric field treatment the crystals show a more narrow orientation distribution as well as a strongly increased (110)-signal of the PPerAcr.
In contrast to the results for MiS195 in RL122 a clear signal of the phase separation is only visible for the melt crystallised sample (Figure 3). The position of these signals is in good agreement to measurements of bulk samples. For the melt crystallised samples a parallel orientation of the cylinders to the substrate was confirmed by atomic force microscopy beforehand.
After the electric field treatment the signal of the phase separation is not visible anymore. One possible explanation could be that the sample had not enough time to form the phase separated structure under the influence of the electric field. Also a degradation of the material under the exposure of the electric field in the molten state could serve as a possible explanation. In addition to the disappearance of the signal from the phase separation also a change in the crystalline orientation was observed.

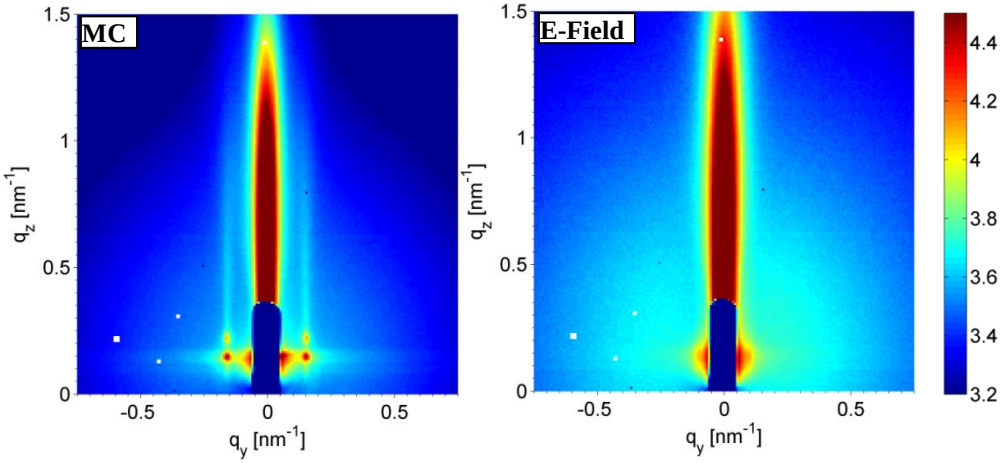

Figure 3: GISAXS data of RL122 after melt crystallisation (left) and electric field treatment (right) (logarithmic scale).

Appendix B

The impact of solvent vapor on the orientation of the cylindrical morphology of P3HT-*b*-PperAcr (RL122) in thin films was investigated. 70 nm films were prepared by spin casting and the difference between thermal treatment and treatment with solvent vapor was investigated and shown with AFM (Fig. 4). After melt crystallization, i.e. heating the film above 255°C for 5 min, microphase separation of the polymer can be observed (Fig. 4a). The cylinders are oriented in such a way that they lie flat on the substrate but they are not highly ordered. After annealing the film in chloroform vapor for 24 h (Fig. 4b) phase separation can also be observed but there appear to be differences in the orientation of the morphology. In addition to the worm like structures seen before, spheres can be observed. This indicates a partial reorientation of the morphology with some of the cylinders oriented perpendicular to the surface.

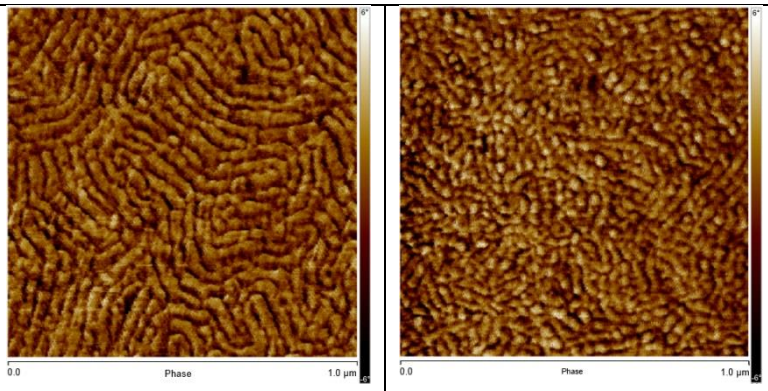

a) **b)**

Figure 4: AFM images of spin cast 70 nm films of P3HT-*b*-PPerAcr. Image **a**) shows the melt crystallized film (i.e. the film was heated above 255°C for 5 min in inert atmosphere) whereas image **b**) shows a film after annealing in chloroform vapor for 24 h.

It was expected that the microphase separation could also be observed in GISAXS measurements. In both films no peaks could be observed though (see Fig. 5a and c). This would either mean that the polymer films are not microphase separated, which is in contradiction to the AFM results, or that the film thickness of 70 nm was insufficient to observe the separation.

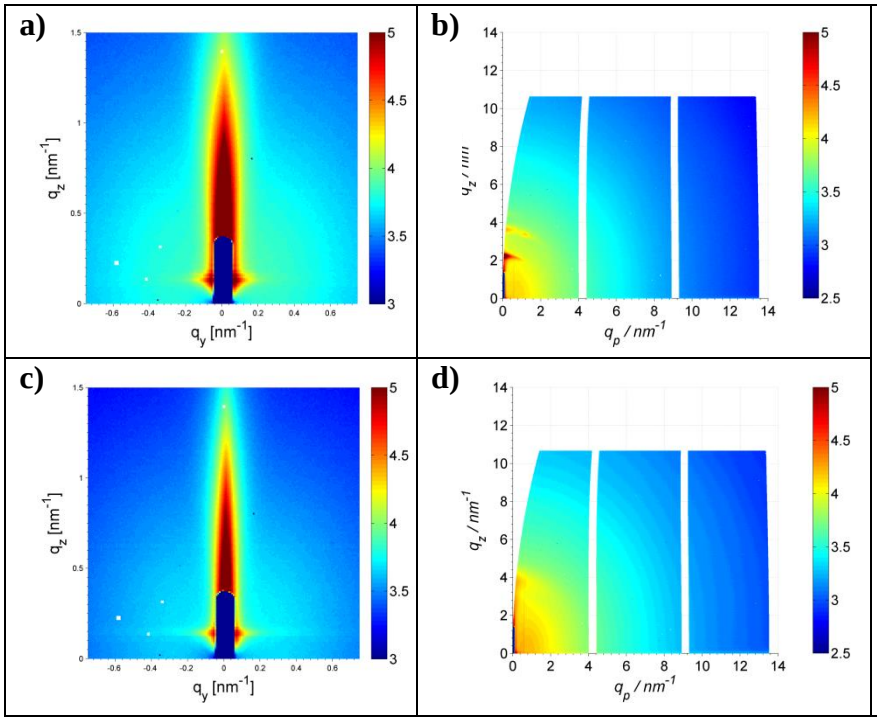

Figure 5: Grazing incidence X-ray measurements of spin cast 70 nm P3HT-*b*-PPerAcr films. GISAXS (**a**) and GIWAXS (**b**) measurements of a melt crystallized film (i.e. the film was heated above 255 °C for 5 min in inert atmosphere). GISAXS (**c**) and GIWAXS (**d**) measurement of a film after solvent vapor annealing in Chloroform for 24 h.

WAXS measurements (Fig. 5 b and d) show a marked difference between the films after thermal treatment or solvent vapor annealing. The peaks in Fig. 5d have a lower intensity and are broader than the ones observed in the thermally treated film (Fig. 5b).Treatment with chloroform therefore leads to a film with lower crystallinity and lower order in contrast to melt crystallization.

Appendix C

From previous measurements on RL 95 films, it is known that PPerAcr exhibits a dominant edge on orientation with the 'a' axis of PPerAcr aligned perpendicular to the substrate. As the GIWAXS geometry does not allow observation of intensity directly on the meridian, i.e. along the q_z axis, exact determination of the crystallite orientation distribution is not possible from the GIWAXS data set alone. To quantify the azimuthal angular dependence of a particular crystallite orientation distribution, scattering patterns in the specular condition were also obtained using the method as described by Baker et al.[3] by tilting the sample

[3] J. Baker, L. Jimison, S. Mannsfeld, S. Volkman, S. Yin, V. Subramanian,A. Salleo, A. Alivisatos, and M. Toney, Langmuir, vol. 26, no. 11, pp. 9146_9151, 2010

such that the angle of incidence is equal to the exit angle $\alpha_i = \alpha_f$ for the dominant (100) reflections from PPerAcr and P3HT. A representative scattering pattern in the GIWAXS geometry and the local specular condition for RL 95 films annealed in the melt state is shown in Figure 6.

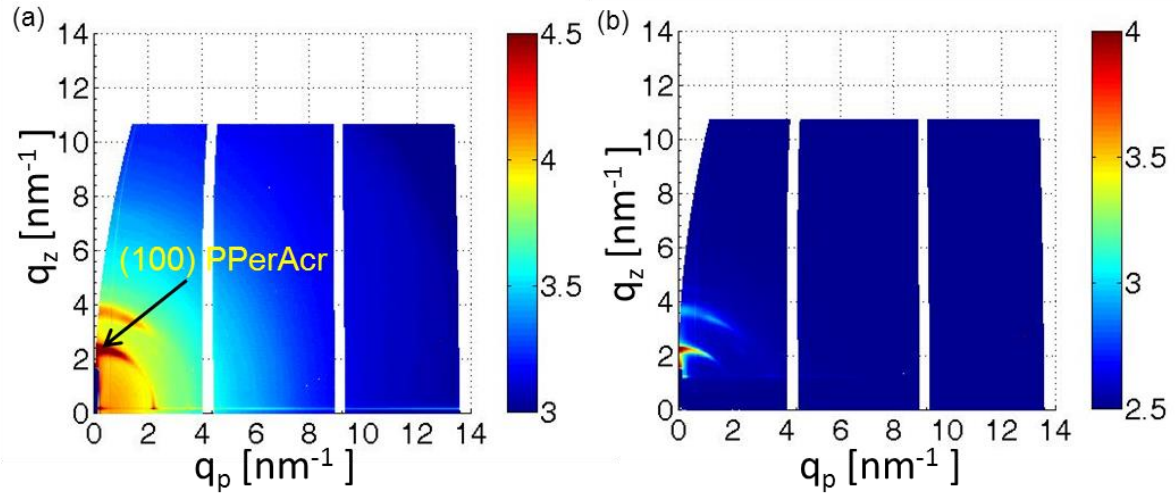

Figure 6: Scattering pattern of P3HT-b-PPerAcr crystallized from the melt with microphase separation in (a) grazing incidence geometry and (b) in specular condition for the (100) reflection from PPerAcr.

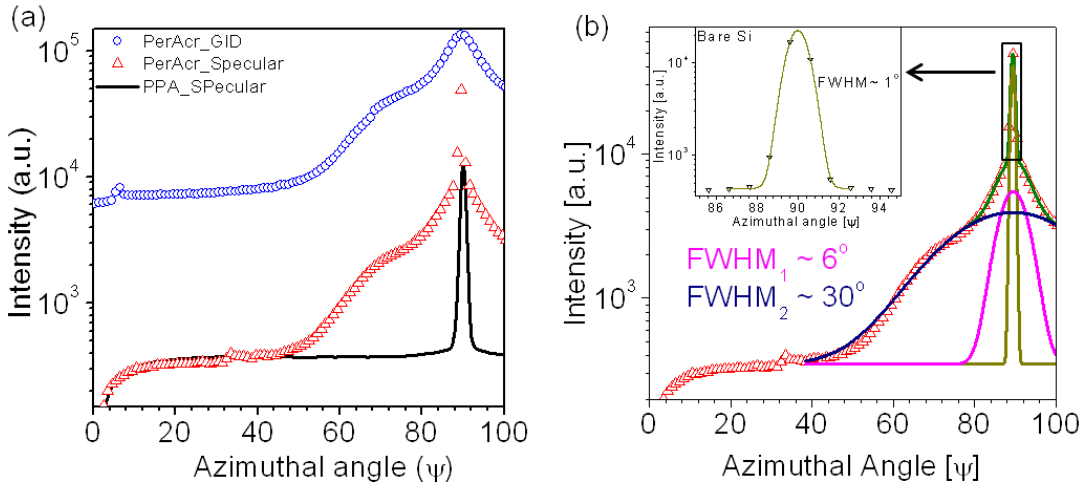

Figure 7: (a) Azimuthal intensity profiles of the (100) PPerAcr reflection from RL95 films (annealed in melt state) in GIWAXS geometry (blue circles) and specular condition (red triangles). The corresponding azimuthal intensity profiles from the bare Si substrate in specular condition for the (100) PPerAcr position (black line) is also shown for comparison. All the data sets were normalized with respect to the exposure time. While, the azimuthal intensity profile for the (100) reflection of PPerAcr in GIWAXS geometry could be fitted with a double gaussian function exhibiting two orientation distribution of crystallites having FWHM of 6° and 30°, the azimuthal intensity profile for the (100) reflection of PPerAcr in specular condition (c) also exhibits two orientation distribution of crystallites having FWHM of 6° and 30°. The additional third peak (FWHM 1°) could possibly originate from the reflected intensity of the layered system (similar to the observed signal of the bare Si substrate) (see inset)

Figure 7a shows the azimuthal intensity profiles of the (100) reflection from PPerAcr in GIWAXS and local specular condition along with the corresponding profile from measurement on Si substrate. The azimuthal intensity profile (GIWAXS) exhibits a large increase in intensity close to the meridian. The profile shows the presence of two peaks, both centered at the meridian, having peak widths (FWHM) of 6° and 30°. The intensity profile of the same reflection in the specular condition (Figure 7c) also reveals the presence of two crystallite orientation distribution at the meridian having similar peak widths (i.e. 6° and 30°) as obtained from the GIWAXS measurement. Additionally, a third peak (FWHM ~ 1°) could also be observed. This resolution limited peak could arise from the reflected intensity of the layered system (organic film and Si substrate). Though, at this point we cannot explicitly rule out the possibility of crystallites which are perfectly oriented (FWHM < 1°), preliminary analysis suggests that scattering patterns in the GIWAXS geometry could possibly be sufficient to provide complete information of crystalline texture in these samples. Further analysis for understanding and interpreting the crystallite orientation quantitatively is underway.

Appendix D

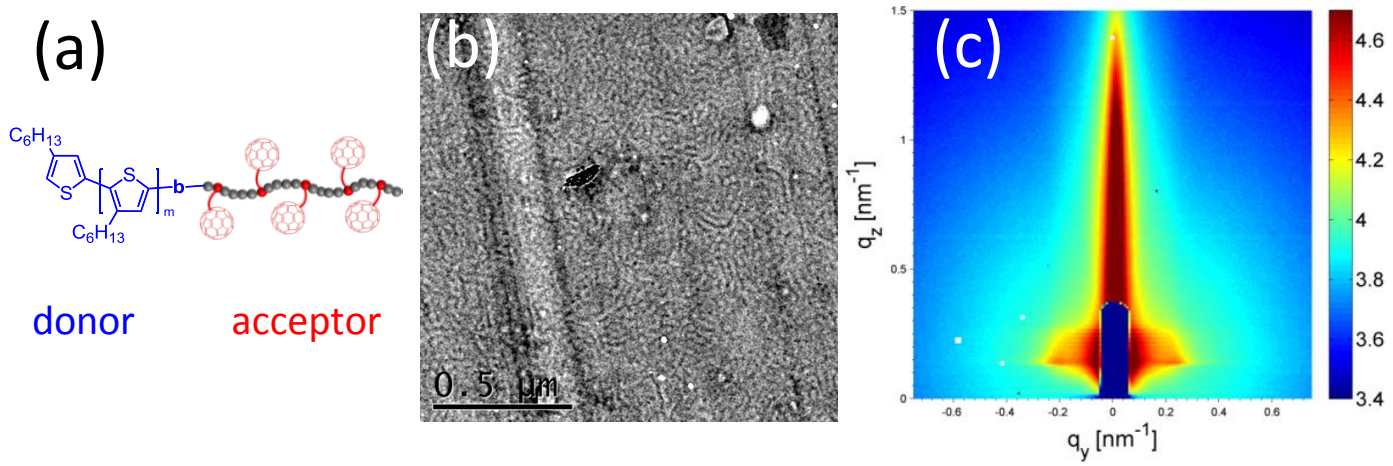

Figure 8: Investigation of a donor-acceptor block copolymer based on poly(3-hexylthiophene) (P3HT) and a $PC_{61}BM$-grafted copolymer block (a). The transmission electron microscopy image of a bulk sample strongly indicates a microphase-separated morphology (b). GISAXS measurement in a melt-crystallized thin film (150 nm) further supports that phase-separation is evident.

Structural investigation of the thin film morphology of a new donor-acceptor block copolymer (P3HT-b-PPCBM) based on poly(3-hexylthiophene) (P3HT) and a fullerene grafted copolymer block PPCBM (Fig. 8a) was done by GISAXS and GIWAXS. Previous studies in our group for this block copolymer by transmission electron microscopy indicate a microphase separation after thermal annealing above the melting temperature of P3HT in bulk samples (Fig. 8b). The new results from GISAXS measurements on a melt-crystallized film shows a distinct GISAXS scattering peak at $q_z = 0.25$ nm^{-1} (Fig. 8c), which correlates with a period of roughly 25 nm. From this we conclude that a microphase separated morphology is also present in melt-crystallized thin films.

Appendix E

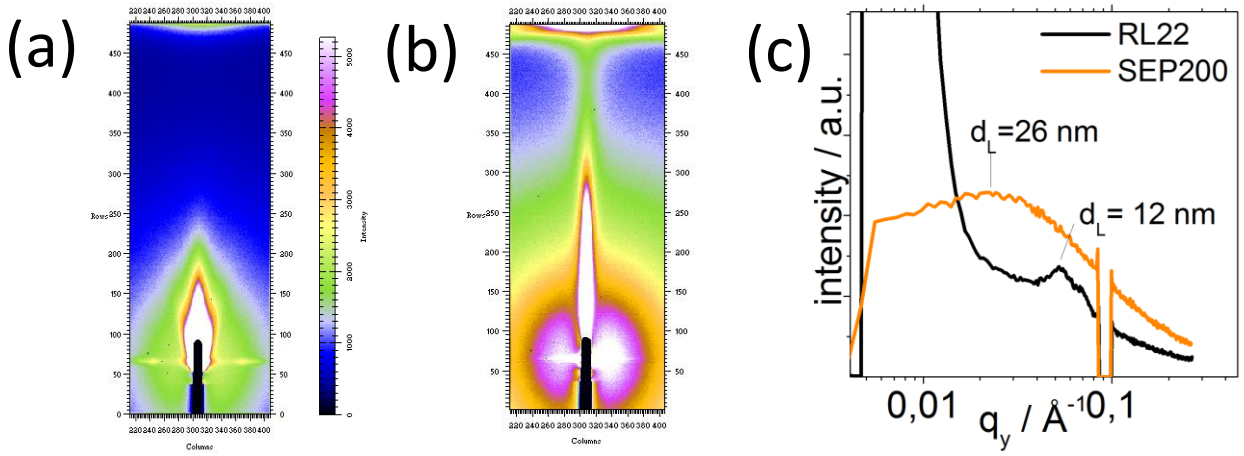

Figure 9: GISAXS patterns of melt-crystallized thin films of (a) the low-molecular weight P3HT RL22 and (b) the commercially available sample SEP200 with corresponding (c) horizontal line cuts in the vicinity of the beam stop.

Previous studies of bulk samples of the semicrystalline polymer P3HT revealed only a weak scattering signal in the small-angle regime corresponding to the semicrystalline morphology (length scale in the order of ~10 nm)[4]. We investigated also thin films with thicknesses in the range of 25 to 200 nm. For the melt-crystallized low-molecular weight sample RL22 we found a clear SAXS signal. In the 2D GISAXS pattern (Fig. 9a) bright spots in the vicinity of the beam stop could be observed. The horizontal line cut shown in Fig. 9c reveals a peak which corresponds to a length of 12 nm. This result is in line with the known long period of the semicrystalline morphology for this sample[4]. In contrast to RL22 for all thin films of high molecular weight P3HTs, e.g. SEP200, we did not observe clearly resolved SAXS signals (see Fig.9b and c).

[4] J. Balko, R.H. Lohwasser, M. Sommer, M. Thelakkat, T.Thurn-Albrecht: Determination of the Crystallinity of Semicrystalline Poly(3-hexylthiophene) by Means of Wide-Angle X‑ray Scattering, Macromolecules, online from 09.12.2013